Search for fermiophobic gauge boson in the dilepton channel with ATLAS, using ATLAS Open Data, $\sqrt{s} = 13$ TeV

Kanhaiya Gupta
Physikalisches Institut, Universität Bonn, Nussallee 12, 53115 Bonn, Germany

Models with extra gauge symmetry were-well motivated extensions of the Standard Model. In this paper, we search for excess of events in search of a heavy neutral gauge boson $Z^{'}$ which is fermiophobic. We are looking at *llbb* final states where the dilepton channel provides the most stringent constraint on the fermiophobic (FB) model. Since, $Z^{'}$ is fermiophobic, the production of such particle can occur via vector boson fusion, with subsequent decays into WW or Zh. We observe no significant excess of events over background only hypothesis and are able to put the constrain on efficiency times cross-section ($\epsilon\sigma$)

I. INTRODUCTION

The Standard Model (SM) of particle physics describes with high accuracy a multitude of experimental and observational data ranging ranging from the smallest energy scales up to the scale of several TeV set by the center-of-mass energy of the Large Hadron Collider (LHC) at CERN. With the recent discovery of the Higgs boson[1, 2], the particle content of the SM corresponds to a renormalizable theory and is in this sense complete. Nevertheless, the SM does not accommodate phenomena such as gravity or dark matter and dark energy inferred from cosmological observations, prompting theoretical work on its extensions. Over the years, many models addressing these shortcomings purport to go "beyond the Standdard Model (BSM)". These models predict new particles in the form of new heavy vector, scalar or fermion resonances which can potentilly be observed at the CERN LHC.

On the earliest BSM scenarios to emerge was Technicolor (TC)[3] but these did not rely on the existence of fundamental scalar particle (Higgs). With the discovery of the Higgs boson at CERN LHC implies the Higgsful extension of the SM. To this end Ref[], constructed a UV completion of the three site model introducing two Higgs doublets to break the gauge symmetries in the way: $SU(2)_L \times SU(2)_R \times U(1)_Y \rightarrow U(1)_{em}$ (which is called 221 model). This extension of the SM predicts the new heavy gauge bosons $W^{'}$ and $Z^{'}$. In addition, it has certain distinguishing features that these $W^{'}$ and $Z^{'}$ are fermiophobic. The fermiophobic particles are the one that do not couple to fermions.

This article presents the search of new heavy neutral gauge boson $Z^{'}$ which is fermiophobic in the dilepton channel using the ATLAS Open Data, 10 fb^{-1} of pp collision at a center-of-mass energy of 13 TeV. More details regarding the motivation for the fermiophobic gauge boson in the di-leptons channel can be found in ref[4]. This paper is organized as follows: In Section 2, we present our search strategy and the searches at the LHC thus far. In Section 3, we present the brief introduction of the ATLAS Detector at the LHC, that has been used to collect the data. In Sec. 3 & Sec. 4, we start with the explanation of the data used and the analysis procedure for the search of the BSM fermiophobic neutral gauge boson. In Sec. 5 and Sec. 6 we estimate the possible sources of background and uncertainties involved. In Sec. 7 & 8, we present our results along with the conclusions.

II. SEARCH STRATEGIES

We begin our search for fermiophobic $Z^{'}$ boson with specific strategy involving the identification of the production and decays of the $Z^{'}$. In the absence of the fermionic couplings, the production of the $Z^{'}$ may proceed via vector boson fusion however, the decay can proceed via multiple mechanism depending on the strength of couplings and the available phase space. In particular $Z^{'}$ decays to Zh, ZW, where h could be SM like Higgs boson or any other heavier scalar particle. Thus, the signal for our search is $pp \rightarrow Z^{'} \rightarrow Zh \rightarrow llbb$, with the Higgs decaying to a pair of bottom quarks and Z decaying leptonically.The $h \rightarrow bb$ channel has large BR, providing strong signal strength where as the dilepton search provides the most stringent constraint, reducing the pure QCD background.

The search for a heavy neutral gauge boson has been performed at both Tevatron and the LHC. The experiment done by CDF and D0 collaboration translated their results for various U(1) extensions of the SM but their analysis did not show any significant excess. The result excluded $Z^{'}$ in the mass range 500-800 GeV, depending upon model specifications.

At the LHC, the ATLAS and CMS experiment have an extensive physics program to search for $Z^{'}$[5, 6]. A

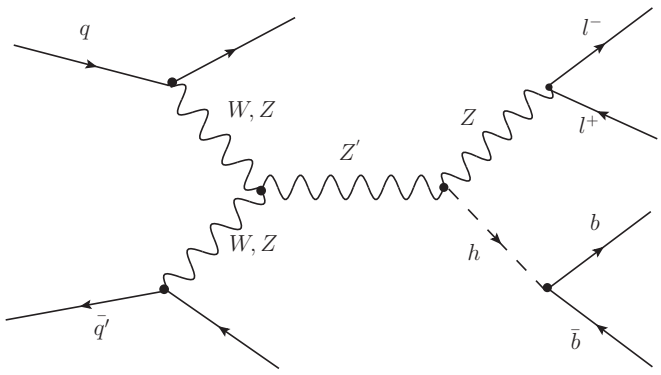

FIG. 1. Feynman diagram showing fermiophobic gauge boson $Z^{'}$ production from the vector boson fusion and its decay to Zh where Z (SM Z boson) decays leptonically, l = e, μ and h (Higgs boson) decays to two b quarks.

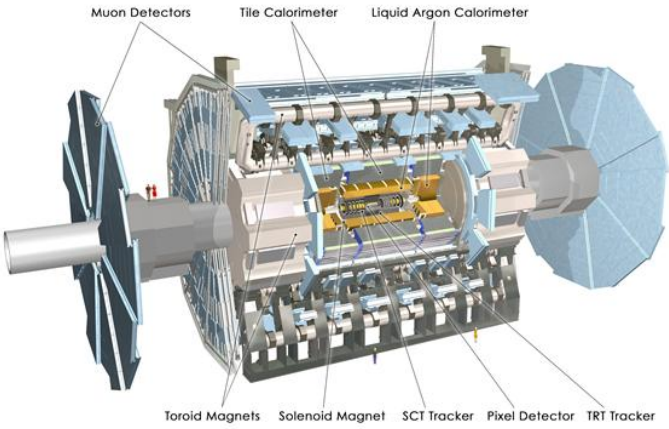

FIG. 2. ATLAS Deterctor at CERN showing different components[8]

widely used model in these searches is the Sequential Standard Model (SeqSM)[7], which predicts a spin-1 neutral boson (Z_{SeqSM}) with SM-like couplings. The strategy pursued in those analyses is a simple and robust dilepton selection targeting production via Drell-Yan (DY) process ($q\bar{q} \rightarrow Z^{'} + 0j$), with high signal acceptance that produces a resonance peak in the reconstructed invariant mass spectrum of the lepton pairs that sits above the background.

TABLE I. Excluded region for $M_{Z'}$ searches at LHC

Collaboration	Luminosity (fb^{-1})	$Z^{'}_{SeqSM}$
CMS-8	20.6	2.9 TeV
CMS-13	2.7	3.37 TeV
ATLAS-13	3.2	3.36 TeV
ATLAS-13	36.1	3.8 TeV

III. ATLAS DETECTOR

The ATLAS Detector[9] is a multipurpose detector at LHC with a forward-backward symmetric cylindrical geometry and nearly 4π coverage in solid angle. It consists of an inner tracking detector surrounded by a thin superconducting solenoid providing a 2 T axial magnetic field, electromagnetic and hadron calorimeters, and a muon spectrometer. The ID includes two silicon subdetectors, namely an inner pixel detector and an outer microstrip tracker, inside a transition radiation tracker (TRT) based on gas-filled drift tubes. The muon spectrometer (MS) surrounds the calorimeters and measures muon tracks within a system of three superconducting air-core toroidal magnets with eight coils each. The MS consists of three layers of precision tracking and triggering chambers. The more details regarding the ATLAS Detector can be found in ref[9].

IV. DATA SAMPLES AND BACKGROUND

The analysis uses the 13 TeV ATLAS Open Data[10] events that belongs to 61 runs from the first four periods of the 2016 pp data-taking. The data-set corresponds to an integrated luminosity of $10.06 \pm 0.37 fb^{-1}$, after data quality requirements have been applied.

The dominant SM background comes from $t\bar{t}$, $t\bar{t}$+jets WZ + jets, ZZ + jets, $Z + jets$ processes. We demand at least 4 jets, exactly two b-quarks and 2 leptons (either e or μ) in the final state, which reduces the background considerably. Background processes were modelled using Monte Carlo (MC) event generators to study kinematic distributions, to evaluate background contamination in the signal region and to interpret the results. WZ & ZZ were modelled using SHERPA 2.2[11], while $t\bar{t}$, $Z + jets$, were modelled using POWHEG-Box v2[12] + Pythia 8[13].

V. ANALYSIS PROCEDURE

A. Reconstruction of electron, muon, and jet candidates

Electron candidates are reconstructed from an isolated electromagnetic calorimeter (EMCAL) energy deposit, matched to the track in the inner tracking detector (InDet), within the ficudial region of $|\eta_{cluster}| < 2.47$ where $\eta_{cluster}$ is the pseudorapidity of the calorimeter energy deposit associated with the electron candidate. Muon candidates are reconstructed by combining tracks reconstructed in both the inner detector and the muon spectrometer (MS). Both electron and muon candidates are required to have $P_T > 7$ GeV and to pass the "loose"

identification criteria to reduce the contribution from non-prompt leptons (e.g. from the semileptonic b- or c-hadron decays), photon conversion and hadrons.

If multiple vertices are reconstructed, the vertex with the largest sum of the squares of the transverse momenta of the associated tracks is taken as the primary vertex of the event: the longitudinal impact parameter z_0 is required to satisfy $|z_0 sin\theta| < 0.5$ mm, where θ is the polar angle of the track.

The jet candidates are reconstructed from three-dimensional topological energy clusters in the EMCAL and hadronic calorimeter (HCAL) using the anti-k_t jet algorithm with a radius paramter of 0.4, and these are referred to as "small-R jets". After energy calibration, all jets candidates are required to have $P_T > 20$ GeV and $|\eta| < 2.5$. To reduce the effect of pileup, and additional requirement is made on the jets with $P_T < 60$ GeV and $|\eta| < 2.4$. Identification of jets containing b-hadrons (b-tagging) is performed with a multivariate discriminant, MV2c10, making use of track impact parameter, the b-hadron flight path inside the jet and reconstructed secondary vertices. For each jet, a value for the multivarite b-tagging discriminant is calculated, and the jet is considered b-tagged if this value is above a given threshold: the so-called algorithm "working point (WP)", which corresponds to a given efficiency to tag a jet containing a b-hadron.

B. Cut selection

The analysis implements the selection criteria for the Zh events, where the Z boson decays into an electron-positron or muon-antimuon pair ($Z \to e^- e^+$ and $Z \to \mu^- \mu^+$), and the Higgs boson (h) decays hadronically to $b\bar{b}$. The leptons are required to pass the tight identification criteria. The final event-selection criteria are:

- Single-electron or single-muon trigger satisfied;
- At least 4 jets events;
- Missing transverse energy < 30 GeV, to reduce the $t\bar{t}$ background.
- Exactly two same-flavour opposite-charge (SFOS) leptons (electrons or muons) with $P_T > 25$ GeV;
- Exactly two b-tagged jets with $MV2c10 > 0.8244273$ which is 70% of "algorithm working point (WP)" with $P_T > 30$ GeV;
- $\Delta R_{bb} = \Delta R_{ll} = \Delta R_{bl} \geq 0.4$;

The basic identification cut on P_T will help to eliminate the soft jets and leptons which arise during hadronization. The $\Delta R \geq 0.4$ ensures that all pair of final states are optimally separated.

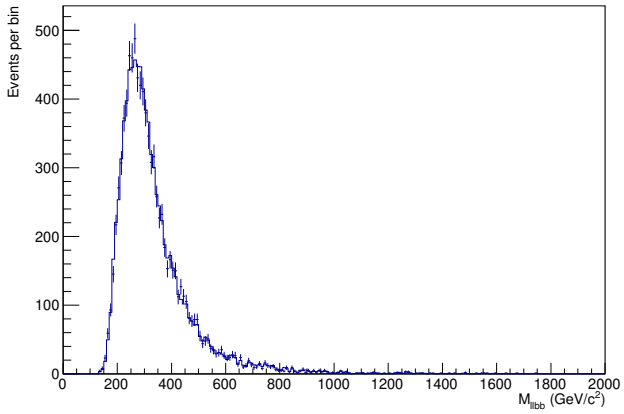

FIG. 3. Fitting the data with MC events using TFraction Fit

TABLE II. MC Sample Fit Fractions results

MC Sample	Fraction	Uncertainty	Expected events at mode
ZZ	0.144382	± 0.04290	79±9
WZ	0.236027	± 0.01690	75±12
$t\bar{t}$	0.567863	± 0.03514	312±19
Z+jets	0.151728	± 0.04290	83±23

C. Kinetic discriminants

We consider important kinetic variables, the transverse momentum of the leading b-jet and lepton, the missing transverse energy ($\not{E}_T$) and various invariant mass. Based on the kinetic variable, we define a control region that has background rich events. Inn the control region, we apply the TFraction Fit[14] to determine the contributions of each of the background on data and hence the scaling factor. Based on this scaling factor, we filled our histograms in the signal region. The background along with data are stacked to see the excess of events over background only hypothesis. And the cut and count technique is applied in case of not significant excess to determine the confidence limit.

VI. UNCERTAINTIES

The systematic uncertainties include those due to the limited numbers of simulated events and to the measurement of integrated luminosity. Experimental uncertainties arising from the trigger efficiencies, lepton and jet identification and reconstruction procedures, the energy calibration of leptons and jets, and b-tagging efficiency.

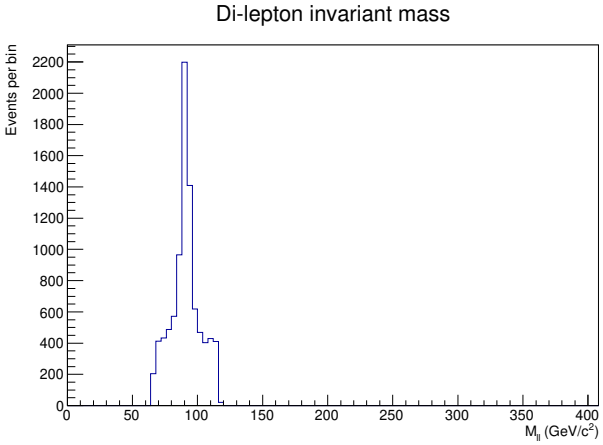

FIG. 4. Invariant mass plot of dilepton(l) , $l = e, \mu$

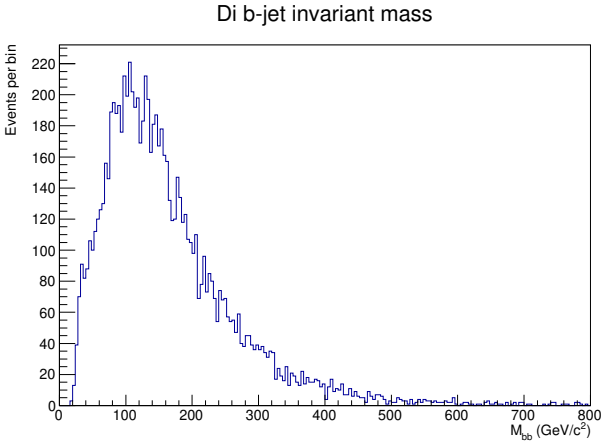

FIG. 5. Invariant mass plot of di-jets

TABLE III. Events passing the cut selection

Cut selection	Data	ZZ + jets	WZ + jets	$t\bar{t}$	Z+jets
Initial	12205790	1403146	1316619	2910539	5446674
Trigger	12205790	1403146	1316619	2910539	5446674
$N_{jets} > 4$	275579	173843	205109	924600	930052
$N_l = 2$	129554	112474	132239	395681	528817
$N_b = 2$	3119	4493	389	19500	29687
$\not{E_T} \leq 30$ GeV	880	2537	195	2375	16913
80 GeV $\leq M_{l_1 l_2} \leq 100$ GeV	195	2364	177	998	15872
100 GeV $\leq M_{b_1 b_2} \leq 140$ GeV	129	270	25	215	3484
600 GeV $\leq M_{l_1 l_2 b_1 b_2} \leq 1000$ GeV	8	15	2	0	48

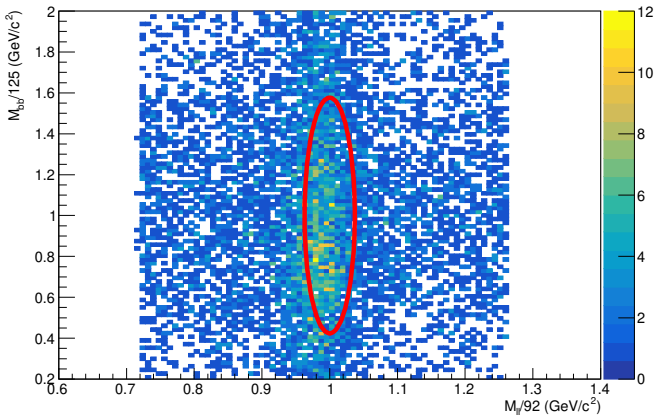

FIG. 6. 2d histogram plot of invariant mass of dileptons against invariant mass of di-bjets. The region inside the red ellipse, display the signal region. The radius of the ellipse are calculated from the half decay width of the reconstructed invariant mass shown in Fig 4 & Fig 5.

VII. RESULTS

We defined a scale factor for each MC samples based on TFraction Fit root class. The fitted results are shown in Tabe II. The defined scale factor matches nicely for the leading transverse momentum of leptons and jets as shown in Fig 7 and Fig 8. We did not observe any excess of events over background only hypothesis as shown in Fig 9.In Table III, we show the number of events passing the various cut selection. In Fig 6, we define the signal region as shown in the red curve. The width of the ellipse axes are taken from the half wdith maxima of the invariant of di-leptons and di-bjets shown in Fig 4 and Fig 5. Based on Bayes theorem, we are able to set limit on $\epsilon\sigma \times BR$. The obtained constrain was $\epsilon\sigma \times BR < 0.25$ fb.

VIII. CONCLUSION

This paper presents search for fermiophobic gauge boson in the di-lepton channel using ATLAS Open Data at $\sqrt{s} = 14$ TeV. The analysis uses TFraction Fit to calculate the fraction of MC samples contributing to the data. No excess of data with respect to SM predictions are observed. Hence, we are able to put a constrain on efficiency times production cross-section times branching ratio. A strong constrain may be put with the high integrated luminosity data.

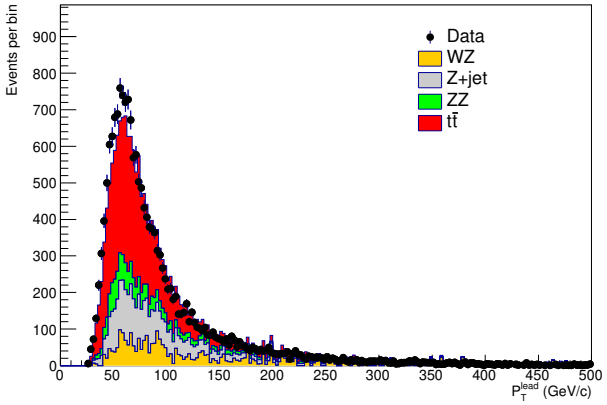

FIG. 7. Comparison between data and MC predictions for the leading transverse momentum for the leptons (P_T^{lead})

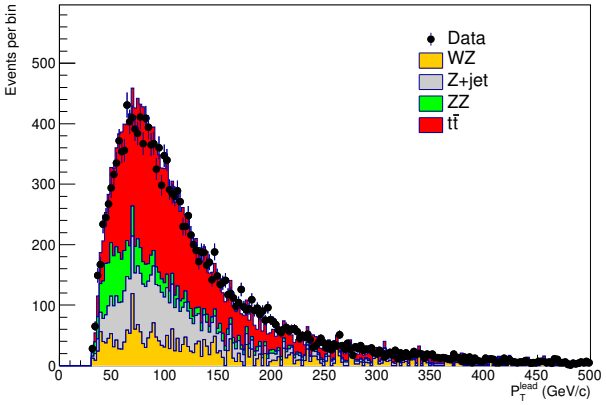

FIG. 8. Comparison between data and MC predictions for the leading transverse momentum for the b-tagged jets (P_T^{lead})

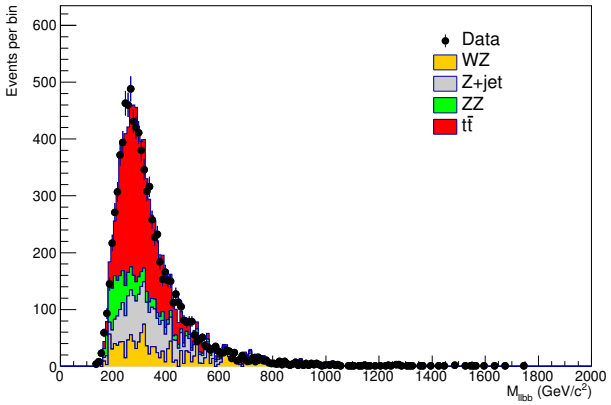

FIG. 9. Comparison between data and MC predictions for the invariant mass of the final states particles ($M_{l_1 l_2 b_1 b_2}$)

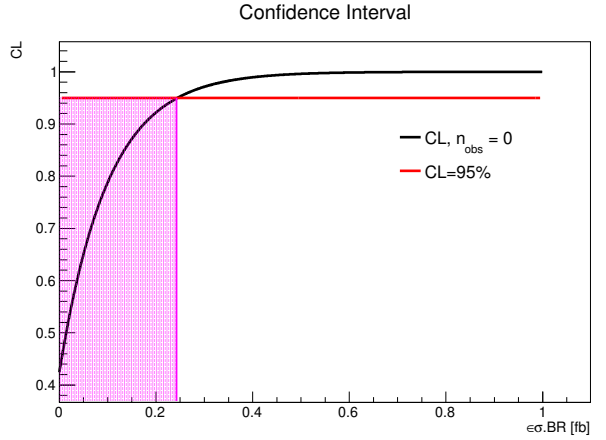

FIG. 10. Plot showing the Confidence level (CL) vs efficiency times production cross-section times branching fractions($\epsilon\sigma \times BR$). The region shown the pinl color is the feasible region and outside that is the excluded. The value $> \epsilon\sigma \times BR$ is excluded.

ACKNOWLEDGEMENT

The author wishes to acknowledge the ATLAS Open Data resources.

[1] G. Aad, T. Abajyan, B. Abbott, J. Abdallah, S. A. Khalek, A. A. Abdelalim, R. Aben, B. Abi, M. Abolins, O. AbouZeid, *et al.*, Observation of a new particle in the search for the standard model higgs boson with the atlas detector at the lhc, Physics Letters B **716**, 1 (2012).

[2] S. Chatrchyan, V. Khachatryan, A. M. Sirunyan, A. Tumasyan, W. Adam, E. Aguilo, T. Bergauer, M. Dragicevic, J. Erö, C. Fabjan, *et al.*, Observation of a new boson at a mass of 125 gev with the cms experiment at the lhc, Physics Letters B **716**, 30 (2012).

[3] C. T. Hill, D. C. Kennedy, T. Onogi, and H.-L. Yu, Spontaneously broken technicolor and the dynamics of virtual vector technimesons, Physical Review D **47**, 2940 (1993).

[4] R. S. Chivukula, B. Coleppa, S. Di Chiara, E. H. Simmons, H.-J. He, M. Kurachi, and M. Tanabashi, A three site higgsless model, Physical Review D **74**, 075011 (2006).

[5] C. Collaboration, F. Canelli, B. Kilminster, T. Aarestad, L. Caminada, A. De Cosa, R. Del Burgo, S. Donato, C. Galloni, A. Hinzmann, *et al.*, Search for narrow resonances in dilepton mass spectra in proton-proton collisions at, Physics Letters B **768**, 57 (2017).

[6] M. Aaboud, G. Aad, B. Abbott, J. Abdallah, B. Abeloos, R. Aben, O. AbouZeid, N. Abraham, H. Abramowicz,

H. Abreu, *et al.*, Search for high-mass new phenomena in the dilepton final state using proton–proton collisions at s= 13tev with the atlas detector, Physics Letters B **761**, 372 (2016).

[7] V. D. Barger, W.-Y. Keung, and E. Ma, Sequential W and Z Bosons, Phys. Lett. B **94**, 377 (1980).

[8] J. Pequenao, Computer generated image of the whole ATLAS detector (2008).

[9] G. Aad, J. Butterworth, J. Thion, U. Bratzler, P. Ratoff, R. Nickerson, J. Seixas, I. Grabowska-Bold, F. Meisel, S. Lokwitz, *et al.*, The atlas experiment at the cern large hadron collider, Jinst **3**, S08003 (2008).

[10] A. Note, Review of atlas open data 8 tev datasets, tools and activities, CERN Note (2018).

[11] E. Bothmann, G. Singh Chahal, S. Höche, J. Krause, F. Krauss, S. Kuttimalai, S. Liebschner, D. Napoletano, M. Schönherr, H. Schulz, and et al., Event generation with sherpa 2.2, SciPost Physics **7**, 10.21468/scipostphys.7.3.034 (2019).

[12] C. Oleari, The powheg box, Nuclear Physics B - Proceedings Supplements **205-206**, 36–41 (2010).

[13] T. Sjöstrand, S. Mrenna, and P. Skands, A brief introduction to pythia 8.1, Computer Physics Communications **178**, 852–867 (2008).

[14] R. Barlow and C. Beeston, Fitting using finite monte carlo samples, Computer Physics Communications **77**, 219 (1993).